doi.org/10.36721/PJPS.2026.39.6.155.1

Comparative pharmacokinetic analysis of curcumin and curcumin O-glucuronide through curcumin nano-gel-based delivery system using liquid chromatogram tandem mass spectrometry

Lue Hong[1#], Ruohan Man[2#], Xiaowan Chen[2], Ziming Yang[2], Dingjie Shen[2] and Wei Chen[2,3,4,5,6*]

[1]The First School of Clinical Medicine, Zhejiang Chinese Medical University, Hangzhou, China
[2]Postgraduate Training Base alliance of Wenzhou Medical University, Zhejiang Cancer Hospital, Hangzhou, China
[3]Zhejiang Cancer Research Institute, Zhejiang Cancer Hospital, Hangzhou, China
[4]Hangzhou Institute of Medicine (HIM), Chinese Academy of Sciences, Hangzhou, China
[5]Key Laboratory of Prevention, Diagnosis and Therapy of Upper Gastrointestinal Cancer of Zhejiang Province, Hangzhou, China
[6]Zhejiang Provincial Key Laboratory of Integrated Traditional Chinese and Western Medicine on Cancer, Hangzhou, China

Abstract: **Background**: Curcumin exhibits limited oral bioavailability owing to its poor solubility and rapid metabolism. **Objectives**: To develop a novel curcumin nano-gel (CNG) and evaluate its pharmacokinetics following oral and rectal administration. **Methods**: A sensitive LC MS/MS method was established for the simultaneous quantification of curcumin and its major metabolite curcumin O glucuronide (COG) in plasma. The pharmacokinetics of CNG were compared with those of curcumin suspension (CS) to evaluate the improvement in oral and rectal absorption. CNG and curcumin suspension (CS) were administered orally (1000 mg/kg) and rectally (200 mg/kg) to mice or rats. Plasma samples were collected, and pharmacokinetic parameters were analyzed using WinNonlin. **Results**: CNG formed well dispersed nanoparticles in water. Oral administration of CNG significantly enhanced curcumin absorption, yielding a 66.7 fold higher C_{max} for curcumin and an 84.8 fold higher C_{max} for COG compared with CS. The AUC of curcumin and COG increased by 9.2 fold and 24.4 fold, respectively. Rectal administration of CNG resulted in a 5.5 fold higher C_{max} and a 3.5 fold higher AUC of curcumin relative to oral CS. **Conclusion**: CNG markedly improves the bioavailability of curcumin via both oral and rectal routes, demonstrating its potential as an effective delivery system for enhancing curcumin therapeutic application.

Keywords: Curcumin; Curcumin O-glucuronide; LC-tandem mass spectrometry; Pharmacokinetics; Rectal suppository

Submitted on 05-05-2025 – Revised on 26-09-2025 – Accepted on 09-10-2025

INTRODUCTION

Curcumin is a yellow colored, low-molecular weight, natural polyphenol extracted from the rhizome of turmeric (Curcuma longa) (Scazzocchio *et al*., 2020, Wang *et al*., 2023). For centuries, it has been used in traditional medicine-particularly in China and India-primarily for treating inflammation and skin wounds (Wang *et al*., 2023, Pei *et al*., 2024, Gong *et al*., 2023, Heidari *et al*., 2023, Li *et al*., 2018). Studies have shown that curcumin exhibits potential therapeutic effects against a wide range of chronic diseases, including cardiovascular, diabetes, asthma, allergies, arthritis, atherosclerosis, neoplastic, inflammatory, neurological, pulmonary, metabolic and psychological diseases (Fu *et al*., 2021, Li *et al*., 2020, Pourbagher-Shahri *et al*., 2021). Owing to its potent anti-proliferative activity, particular interest has been directed toward its chemopreventive and chemotherapeutic potential in human cancers (Pooresmaeil and Namazi, 2020). *In vitro* studies have demonstrated that curcumin can inhibit carcinogenesis in various cancer types, such as prostate, lung, colon, ovarian, breast, head and neck, cervical, gastric, hepatic, leukemia and pancreatic cancers (Ma *et al*., 2019, Zoi *et al*., 2024).

Clinically, curcumin has been shown to be extremely safe even when administered at very high doses, with significantly milder side effects compared to conventional anticancer drugs. Despite its attractive medicinal properties and broad therapeutic potential, the clinical application of curcumin is substantially limited by its poor oral bioavailability (Pei *et al*., 2024, Yavarpour-Bali *et al*., 2019). Its hydrophobic nature resulting in water insolubility under acidic conditions and rapid degradation in neutral/alkaline environments, exhibiting a remarkably short half-life ($t_{½}$) less than 10 min in PBS at pH 7.2. The maximum solubility of curcumin in aqueous buffer at pH 5.0 has been reported to be only 11 ng/mL (Gupta and Dixit, 2010). Thus, various organic solvents are commonly used in experiments to enhance solubility (Zhang *et al*., 2019). Studies reported that absorbed curcumin in rodents undergoes rapid first-pass metabolism and biliary excretion (Hassanzadeh *et al*., 2020a). In summary, the oral bioavailability of curcumin is constrained by its extremely low aqueous solubility at physiological pH, extensive

*Corresponding author: e-mail: chenwei@zjcc.org.cn
#These authors contributed equally to this work.

intestinal and hepatic metabolism, rapid elimination and chemical instability under alkaline conditions. Furthermore, solubilized curcumin is sensitive to UV light and may undergo photodegradation during handling (Onoue *et al*., 2010).

Contemporary research efforts in curcumin are predominantly directed toward pharmaceutical and medicinal chemistry strategies designed to improve its aqueous solubility, chemical stability and bioavailability while enabling controlled drug delivery specifically to cancerous tissues (Lübtow *et al*., 2017, Yavarpour-Bali *et al*., 2019, Li *et al*., 2018). These strategies include encapsulating curcumin within liposomes, phospholipids, solid lipid microparticles, cyclodextrins, hydrogels, or nanoparticles, as well as incorporating it into transdermal films, microspheres and nano-emulsions. Additionally, the synthesis of structural analogs of curcumin represents another promising direction (Zhang *et al*., 2018, Maleki Dizaj *et al*., 2022).

In this study, the curcumin nano-gel (CNG) was prepared in both oral and rectal suppository formulations and tested *in vitro* and *in vivo*. The physicochemical characteristics of CNG such as morphology, particle size, zeta-potential and stability were investigated. The cytotoxicity of CNG was evaluated against cancer cells. An LC-MS/MS method was developed and validated to simultaneously quantify curcumin and COG in plasma samples. The pharmacokinetic profile of CNG was investigated in mice and rats and compared with that of a conventional curcumin suspension.

MATERIALS AND METHODS

Materials

Curcumin powder was obtained from Acros organics (USA). Curcumin O-glucuronide (COG) was purchased from Sigma-Aldrich. Polyethylene glycol (PEG) 600, Tween 20 and hesperetin were purchased from Aladdin (Shanghai, China). Hydroxypropyl carboxymethyl cellulose (HPCMC) was purchased from Sigma-Aldrich. HPLC or mass spectrometric grade organic solvents including acetonitrile, ethyl acetate, methanol and formic acid etc. were obtained from Fisher Scientific.

Preparation of liquid and solid CNG, curcumin suspension (CS) and curcumin solution

For liquid CNG preparation, curcumin and PEG 600 were placed together in an aluminum foil-covered glass tube and heated to 100°C on a metal heating block. The glass tube was vortexed every 5 mins until curcumin and PEG 600 became a clear solution. Then, Tween 20 was added into the glass tube to make a final concentration of curcumin at 80 mg/mL or 200 mg/mL and ratio of PEG 600/Tween 20 at 4:1 (v/v). For solid CNG preparation, PEG 1500 was used instead of PEG 600 following above protocol. The melted solid CNG was infused to rectal suppository mold and cooled down until it solidified. Curcumin suspension (80 mg/mL) was prepared in 1% hydroxypropyl carboxymethyl cellulose water solution. The suspension was well shaken before every use. Curcumin was dissolved in dimethylsulfoxide (DMSO) to make a 50 mM stock solution for cell culture test.

Cell lines and culture

Cancer cells were cultured at 37°C in a humidified 5% CO_2 atmosphere, using Dulbecco's modified Eagle's medium (DMEM) or RPMI 1640 supplemented with 10% FBS (Gibco) and 1% (v/v) penicillin-streptomycin (Gibco).

In vitro cytotoxicity evaluation and comparison of curcumin in different formulations

The cytotoxicity evaluation of curcumin formulations (CNG and curcumin-DMSO solution) was conducted in 96-well plates using three cancer cell lines: adherent breast cancer cells MCF-7 (3000 cells/well) and MDA-MB-231 (2500 cells/well), along with suspension leukemia MV4-11 (10,000 cells/well). Following cell-specific culture protocols, breast cancer cells in DMEM medium underwent 24-h adhesion prior to curcumin treatment, while MV4-11 cells in RPMI 1640 medium received immediate compound exposure post-seeding. Dose-dependent cytotoxicity was assessed through MTS assay, with IC_{50} determination performed for both solvent systems.

Transmission electron microscopy (TEM) of CNG

Transmission electron microscopy (TEM) imaging of liquid CNG dilutions was performed using an FEI Tecnai G2 Spirit microscope operating at 80 kV. Briefly, an aqueous CNG solution (0.26 mg/mL) was deposited onto a membrane-coated grid. A drop of 1% uranyl acetate solution was immediately applied. After one minute, excess fluid was blotted with filter paper and the grid was air-dried at room temperature prior to microscope loading.

Dynamic light scattering (DLS) characterization of CNG

Dilution of CNG in water was made and submitted for DLS, polydispersity index (PDI) and zeta-potential determination with a Malvern Zetasizer Nano ZS instrument. Three measurements were performed for each sample.

Stability study of curcumin in CNG

Stability of curcumin in CNG was determined using a spectrophotometer. CNG was prepared as described above at concentration of 200 mg/mL and then was divided into two groups (three tubes per group). One was kept at room temperature and another one was kept in 37°C water bath. Light was protected during the whole experiment. The concentration of curcumin was determined at day 1, 15, 31 and 61. In brief, an aliquot of CNG was diluted 1000 times with pure ethanol. 50 µL of the above solution was

transferred to 96-well plates and the absorption was measured by a Multiskan Spectrum microplate reader (Thermo Scientific) at 425 nm. The concentration of curcumin in CNG was determined based on the constructed calibration curves of curcumin in ethanol.

Construction of calibration curves and preparation of quality controls for LC-MS/MS analysis

Stock solutions of curcumin (1 mg/mL in acetonitrile) and COG (1 mg/mL in methanol) were stored at -80°C. Serial dilutions in 50% acetonitrile/0.1% formic acid aqueous solution generated working standards (20-10,000 ng/mL). For calibration standards, 10 μL aliquots of these solutions were combined with 10 μL hesperetin (I.S., 10 μg/mL) in 10 μL mouse plasma, followed by acidification with 90 μL phosphate buffer (pH 3.2, 0.1 M). Quality control (QC) samples (2.0, 5.0, 50, 500 ng/mL) underwent identical processing. Liquid-liquid extraction was performed using 600 μL ethyl acetate with centrifugation (12,000 rpm, 1 min). The organic phase was transferred, nitrogen-evaporated and reconstituted by addition of 100 μL 50% acetonitrile/0.1% formic acid. After secondary centrifugation (12,000 rpm, 5 min), supernatants were submitted for LC-MS/MS analysis.

Detection of curcumin and COG in plasma by LC-MS/MS

10 μL I.S. was spiked into 10 μL plasma sample and acidified by adding 90 μL phosphate buffer (0.1 M, pH 3.2) and followed by ethyl acetate extraction as described above. 25 μL of reconstituted sample was submitted for LC-MS/MS analysis.

Stability study of COG in mouse plasma

COG working solution was added into mouse plasma to make concentrations of 2 and 10 μg/mL and then the mouse plasma was incubated in 37°C water bath, withdrawn and stored at -80°C freezer immediately at designed time points.

Recovery and matrix effects

A post-extraction recovery and matrix effect assessment was conducted for curcumin, COG and I.S. (1 μg/mL) in mouse plasma using ethyl acetate extraction. Three sample groups (A-C) were prepared at concentrations of 5, 50 and 500 ng/mL for curcumin/COG: Group A contained analytes directly dissolved in 50% acetonitrile/0.1% formic acid; Group B consisted of analytes spiked into reconstituted blank plasma extracts; Group C comprised reconstitution of pre-extracted analytes from plasma. Recovery rates were determined by comparing Group C to Group B peak areas, while matrix effects were evaluated through Group B versus Group A peak area ratios.

Validation of the LC-MS/MS method

The method validation protocol included intra-day (n = 6) and inter-day (triplicate runs across three days) assessments at four concentration levels (2, 5, 50, 500 ng/mL). Calibration curves were generated through unweighted linear regression. Precision, defined as the coefficient of variation (CV%) calculated from replicate measurements and accuracy, assessed by comparison of measured mean concentrations to nominal concentrations, were expressed and evaluated, respectively. The LLOQ was defined as the lowest calibrator meeting dual criteria: acceptable accuracy/precision in back-calculated values and a signal-to-noise ratio exceeding 10:1 for analyte peaks.

HPLC and MS conditions

The chromatographic separation was conducted using a Shimadzu HPLC system equipped with four modules: system controller (CBM-20A), pump (LC-20AD), SIL-autosampler (20AC) and degasser (DGU-20A5). Analyte separation was achieved on a Thermo Hypersil-Keystone BetaBasic C8 analytical column (2.1×50 mm, 5 μm) coupled with a guard column (2.1×10 mm, 2 μm), with isocratic elution (50% acetonitrile/0.1% formic acid in water) at 0.2 mL/min flowrate.

Mass spectrometric detection was performed on a Thermo Scientific TSQ Quantum EMR triple quadrupole instrument equipped with an electrospray ionization (ESI) source operating in positive ion mode. Key parameters were set as follows: argon collision gas pressure, 1.5 mTorr; spray voltage, 4900 V; sheath gas flow rate, 49 arbitrary units; capillary temperature, 325°C. Analytes were quantified in multiple reaction monitoring (MRM) mode using the following transitions and collision energies: curcumin, m/z 369→m/z 177 at CE 20%; COG, m/z 544→m/z 369 at CE 15%; IS, m/z 303→m/z 177 at CE 20%. Instrument optimization was achieved via direct infusion of curcumin. System control and data processing were performed using Xcalibur software (version 1.4 SR1).

The pharmacokinetics of oral administration of CNG and CS in mice and rats

Male CD2F1 mice (~20 g, Charles River Laboratories) received 1000 mg/kg curcumin equivalents via oral gavage (250 μL/mouse adjusted by body weight) of either CNG or CS suspended in 1% HPCMC. The blood was collected by cardiac puncture under CO_2 anesthesia occurred at predetermined intervals (0-24 h post-dose). All animal procedures were conducted in accordance with the ethical approval granted by the Institutional Animal Care and Use Committee (IACUC) of Zhejiang Cancer Hospital. Male Sprague-Dawley rats (~200 g, Shanghai SLAC) were dosed rectally with 200 mg/kg curcumin equivalents (200 mg CNG or 200 μL CS in 1% HPCMC). Serial blood samples were obtained through retro-orbital puncture (0-6 h post-dose). All heparinized blood samples were immediately centrifuged at 1000 ×g for 5 min at 4°C. Plasma aliquots were stored at -80°C until LC-MS/MS analysis of curcumin and COG concentrations using the validated method described previously. Pharmacokinetic parameters were derived through WinNonlin software

(v5.0, Pharsight) using appropriate pharmacokinetic models.

Determination of curcumin concentration in mouse and rat plasma

For LC-MS/MS analysis, 10 µL of plasma samples (CNG or CS formulations) were combined with 10 µL of I.S. solution (10 µg/mL in 50% acetonitrile). The mixture was then acidified with 90 µL of 0.1 M phosphate buffer (pH 3.2) and processed following the established sample preparation protocol. Finally, 25 µL of the reconstituted sample was analyzed by LC-MS/MS system.

Statistical analysis

Statistical analyses utilized Minitab software, with data normality and variance homogeneity confirmed via residual plots. Comparative analyses employed: Kruskal-Wallis ANOVA with Dunn's post-hoc test for temporal concentration profiles of curcumin and COG after CNG/CS administration and two-tailed Mann-Whitney U test for formulation comparisons (CNG vs. CS). Results are presented as mean ± SD ($n \geq 3$), with statistical significance defined as $p < 0.05$ in all experiments.

RESULTS

LC-MS/MS analysis of curcumin and COG

Quantification of curcumin and COG was performed using triple-quadrupole LC-MS/MS operating in positive ion mode. Standard solutions of COG (10 µg/mL in 50% acetonitrile/0.1% formic acid) were directly infused into the ESI source at a flow rate of 0.2 mL/min. Full scan analysis identified a predominant $[M+H]^+$ ion at m/z 545. Collision-induced dissociation of this precursor ion yielded a characteristic fragment at m/z 369, corresponding to glucuronic acid cleavage (Fig. 1). After optimizing collision energy to maximize fragment ion intensity, the transition m/z 545→369 was selected for MRM quantification. Proposed molecular structures and fragmentation pathways are illustrated in Fig. 1.

Chromatographic separation demonstrated distinct retention behaviors reflecting compound hydrophilicity: COG, which contains a glucuronic acid group, eluted first at 1.53 min, followed by the I.S. at 1.90 min and curcumin at 3.04 min on the a C8 column (Fig. 2). Although COG and the I.S. co-eluted within the range of approximately 1.5–1.9 min, baseline resolution was achieved through selective mass detection using unique MRM transitions. Specificity of the method was confirmed by evaluating plasma matrix spiked with 2 ng/mL of both curcumin and COG, with no interfering peaks detected in the analyte channels. The observed elution order (COG < I.S. < curcumin) aligns with relative hydrophobicity, where the increased polarity of COG is attributable to its glucuronide group.

Method development and validation

Sample extraction was performed based on a method described (Vijaya Saradhi *et al*., 2010) with modifications. Ethyl acetate was employed to extract the analytes from mouse plasma. The presence of a glucuronic acid moiety in COG confers a significantly lower pKa compared to native curcumin. As previously reported, the recovery rate of curcumin from neutral pH mouse plasma is approximately 40% from neutral pH mouse plasma (Vijaya Saradhi *et al*., 2010). However, without acidification, the recovery of COG from the same matrix is considerably lower. Given that curcumin remains stable only under acidic conditions (pH 3.0–6.5) (Song *et al*., 2011) and the stability of curcumin can be improved by lowering the pH (Vareed *et al*., 2008), the mouse plasma samples was adjusted to pH 3.2 using phosphate buffer before ethyl acetate extraction. An acidic microenvironment has been shown to favor curcumin stability (Wei *et al*., 2020). Curcumin degrades more slowly in acidic aqueous solutions compared to alkaline or neutral environments. Similarly, emulsions of curcumin exhibit reduced decomposition at pH 3.0 relative to alkaline conditions (Kharat *et al*., 2017). Acidification not only improved the recovery of COG but also enhanced the stability of both analytes, particularly curcumin. Method validation results demonstrated excellent linearity ($r^2 > 0.99$) across the 2.0-2000 ng/mL range for both curcumin and COG. Precision and accuracy met FDA GLP requirements, as evidenced by intra-day (six replicates) and inter-day analyses at four concentration levels (2, 5, 50, 500 ng/mL). The LLOQs were determined at 1 ng/mL for curcumin and 2 ng/mL for COG. However, the coefficient of variation (CV%) for curcumin at 0.5 ng/mL and COG at 1 ng/mL exceeded 20%, which is beyond the acceptable limit. Comprehensive validation data, including percentage RSD values in mouse plasma and cell medium matrices, are provided in Table 1.

Matrix effects and extraction recoveries were systematically evaluated at three concentrations levels (5, 50, 500 ng/mL) for all analytes in accordance with current FDA M10 bioanalytical method validation and study sample analysis guidance. The internal standard demonstrated consistent performance with matrix effects of 95-98% and recoveries of 93-97%. For the target analytes, curcumin showed matrix effects of 95-101% and recoveries of 49-57%, whereas COG exhibited matrix effects of 97-111% with recoveries of 36-48%, as summarized in Table 1.

Preparation and characterization of CNG and CS

As previously reported, the solubility of curcumin in aqueous solution is in ng/mL range. This extremely poor solubility is one of the major factors contributing to its low bioavailability. The primary challenge we addressed was enhancing the solubility of curcumin. In our PEG 600/Tween 20-based system, the solubility of curcumin reached 200 mg/mL, which is extraordinarily higher than curcumin’s aqueous solution.

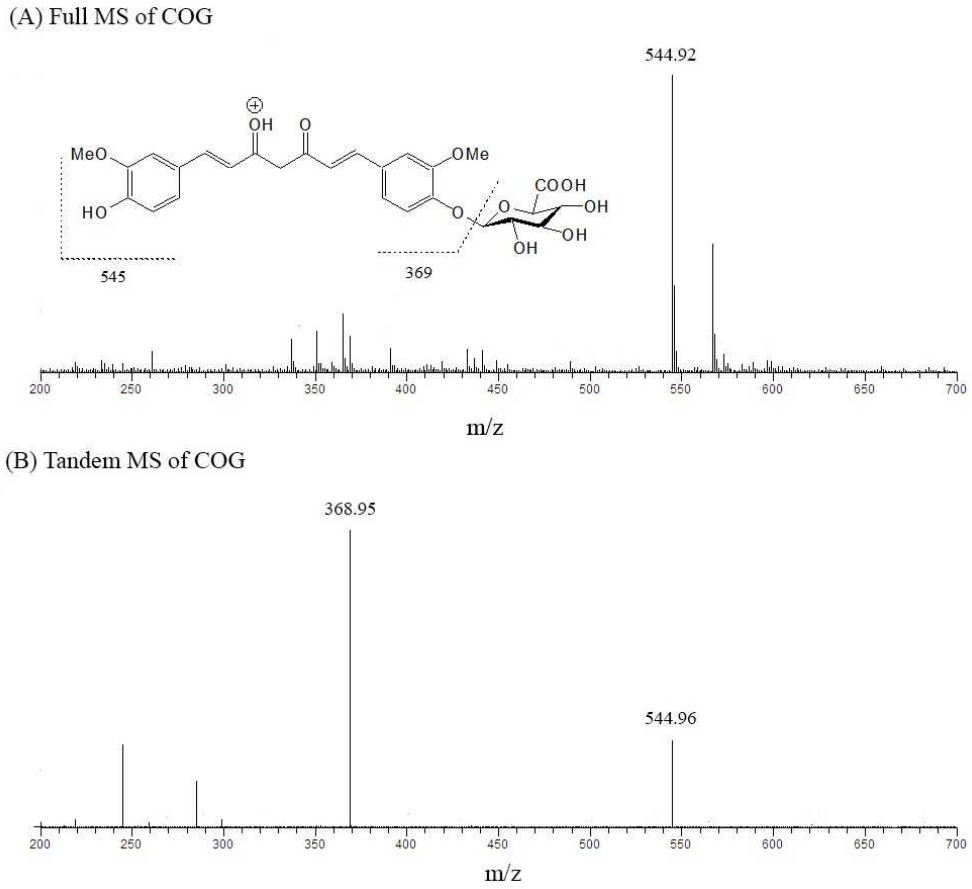

Fig. 1: Mass spectra of COG.

The average 1-min full mass spectrum of COG (10 µg/mL) in 50% ACN/0.1% formic acid showed a base ion at m/z 544.92 (A), corresponding to its protonated molecular ion $[M+H]^+$; (B) the average 1-min product ion spectrum of the ion of 544.9 showed a base ion at m/z 368.95, a product ion generated by cleavage of the glucuronic acid from COG.

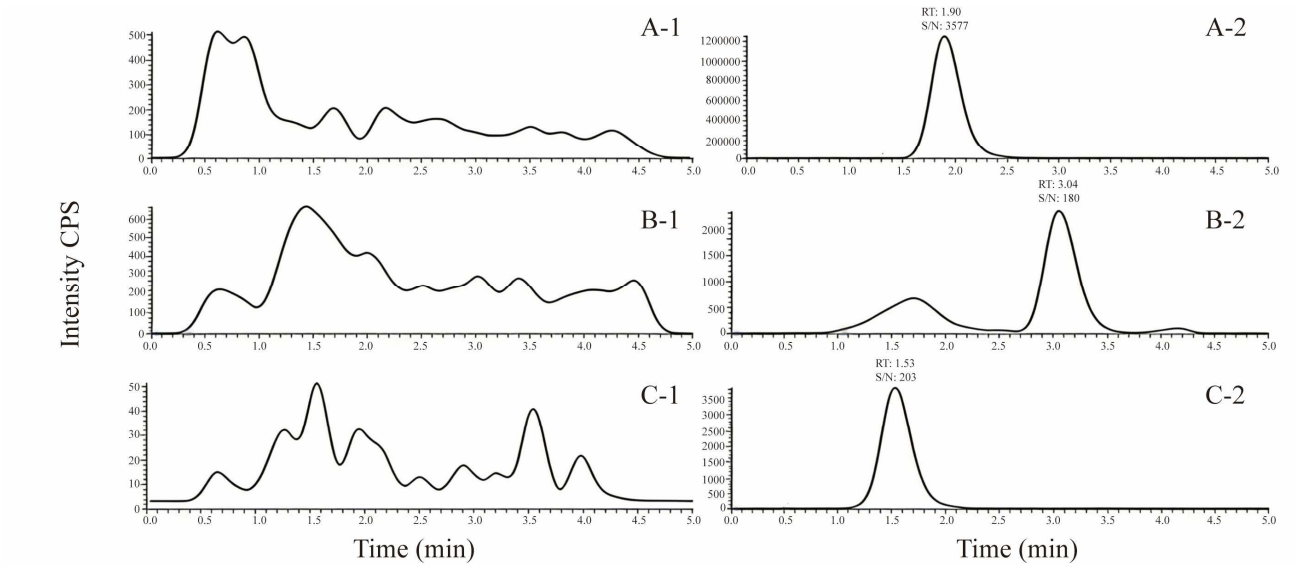

Fig. 2: The chromatograms of curcumin, COG and the internal standard.

Extracted ion chromatograms of mouse plasma spiked with 1000 ng/mL I.S., 2 ng/mL curcumin and COG are shown in A-2, B-2 and C-2, respectively. A-1, B-1 and C-1 are the corresponding extracted ion chromatograms of the analytes in blank in mouse plasma. The retention time of I.S., curcumin and COG are 1.90, 3.04, 1.53 min, respectively. RT: Retention time, SN: signal to noise ratio.

Table 1: Intra-day and inter-day validation of curcumin (A) and COG (B) in mouse plasma.

A

Curcumin (ng/mL)	Recovery (%)	Matrix effects (%)	Intra-day			Inter-day		
			Mean ± S.D.	C.V. (%)	Accuracy (%)	Mean ± S.D.	C.V. (%)	Accuracy (%)
2	N.D.	N.D.	2.37 ± 0.11	4.55	118.67	2.06 ± 0.13	6.19	102.97
5	158.65	27.88	4.44 ± 0.45	10.11	88.79	5.08 ± 0.32	6.24	101.53
50	97.72	36.52	52.16 ± 7.40	14.19	104.32	50.77 ± 6.65	13.10	101.54
500	36.18	96.81	527.00 ± 67.66	12.83	105.46	507.17 ± 64.88	12.79	101.43

B

COG (ng/mL)	Recovery (%)	Matrix effects (%)	Intra-day			Inter-day		
			Mean ± S.D.	C.V. (%)	Accuracy (%)	Mean ± S.D.	C.V. (%)	Accuracy (%)
2	N.D.	N.D.	2.12 ± 0.18	8.70	105.86	1.94 ± 0.25	12.76	97.00
5	126.01	31.95	4.27 ± 0.61	14.21	85.46	4.86 ± 0.56	11.46	97.13
50	72.46	58.08	46.83 ± 6.54	13.97	93.66	53.80 ± 4.17	7.75	107.60
500	41.96	88.91	536.55 ± 64.17	11.96	107.31	515.87 ± 24.07	4.67	103.17

N.D., not determined

Furthermore, the curcumin nano-gel (CNG) formed a homogeneous suspension upon dilution with water.

The morphology of CNG and CS, each containing 80 mg/mL curcumin, along with their diluted forms, is shown in Fig. 3A&C. When CNG was diluted in water to curcumin concentrations of 0.8, 1.6 and 3.2 mg/mL, a homogeneous suspension was obtained. In contrast, dilutions of CS at the same concentrations exhibited much lighter color and obvious curcumin precipitation. Transmission electron microscopy (TEM) images of diluted CNG revealed well-dispersed nanoparticles (Fig. 3B). Dynamic light scattering measurements using a Zetasizer indicated a mean particle diameter of 505.6 ± 29.8 nm, and the particle sizes ranged from 255 nm to 955 nm, a distribution consistent with TEM observations (Fig. 3D). The polydispersity index (PDI) and zeta potential were determined to be 0.2537 ± 0.0175 and -2.727 ± 0.057 mV, respectively. The physical stability of CNG was assessed over two months at both room temperature and 37°C. Throughout this period, the color of the gel remained unchanged. After two months of storage, the decomposition rates of curcumin in CNG were 2.4 ± 2.5% at room temperature and 10.7 ± 1.6% at 37°C (Fig. 4).

Stability of COG in mouse plasma

Although the stability profile of curcumin in mouse plasma has been established by Saradhi *et al*. (Vijaya Saradhi *et al*., 2010), the stability of its glucuronide metabolite (COG) in this matrix remains unexplored. As one of the major metabolites of curcumin, COG demonstrates promising anticancer properties. Therefore, investigating its stability in mouse plasma is valuable for both analytical method development and the evaluation of its pharmacological activity in biological systems. We examined the stability of COG in mouse plasma at 37°C at two concentrations (2 and 10 μg/mL). Samples were analyzed at seven time points over 24 hours using a validated LC-MS/MS method. Corresponding chromatograms of matrix, COG and the I.S. were shown in Fig. S1. The half-life ($t_{1/2}$) of COG at these concentrations was determined to be 1381 min and 2301 min, respectively (Fig. 5). These results indicate that COG is relatively stable compared to curcumin.

In vitro cytotoxicity evaluation and comparison of curcumin in different formulations

The cytotoxicity of curcumin in different formulations against cancer cells was evaluated and compared. In addition to the liquid curcumin nano-gel (CNG), curcumin was also prepared in DMSO, the most commonly used organic solvent for dissolving hydrophobic compounds in cell culture. Equivalent concentrations of curcumin from both CNG and DMSO solutions were tested against MCF-7, MDA-MB-231 and MV4-11 cells. Following a 72-hour treatment period, cell viability was assessed using the MTS assay. Dose-response curves were generated and IC_{50} values were calculated accordingly. Curcumin formulated in CNG exhibited cytotoxicity against all three cancer cell lines comparable to that of the DMSO-dissolved curcumin (Fig. 6, Table 2). Notably, the IC_{50} values for CNG were consistently lower than those for the DMSO solution, suggesting that the CNG formulation may slightly enhance the anticancer activity of curcumin compared to the traditional DMSO-solubilized form.

Pharmacokinetics of orally administered CS and CNG in mice

A comparative pharmacokinetic analysis of liquid CNG and CS was performed in CD2F1 mice following oral administration at a dose of 1000 mg/kg curcumin. Using a validated LC-MS/MS method, the $AUC_{(0\rightarrow 24h)}$ for CNG was determined to be 319 μM·min, compared to 34.57 μM·min for CS, representing a 9.2-fold improvement in oral bioavailability. Additionally, the C_{max} value for CNG was 66.9-fold higher than that of CS (7.02 μM vs. 0.105 μM) (Fig. 7, Table 3).

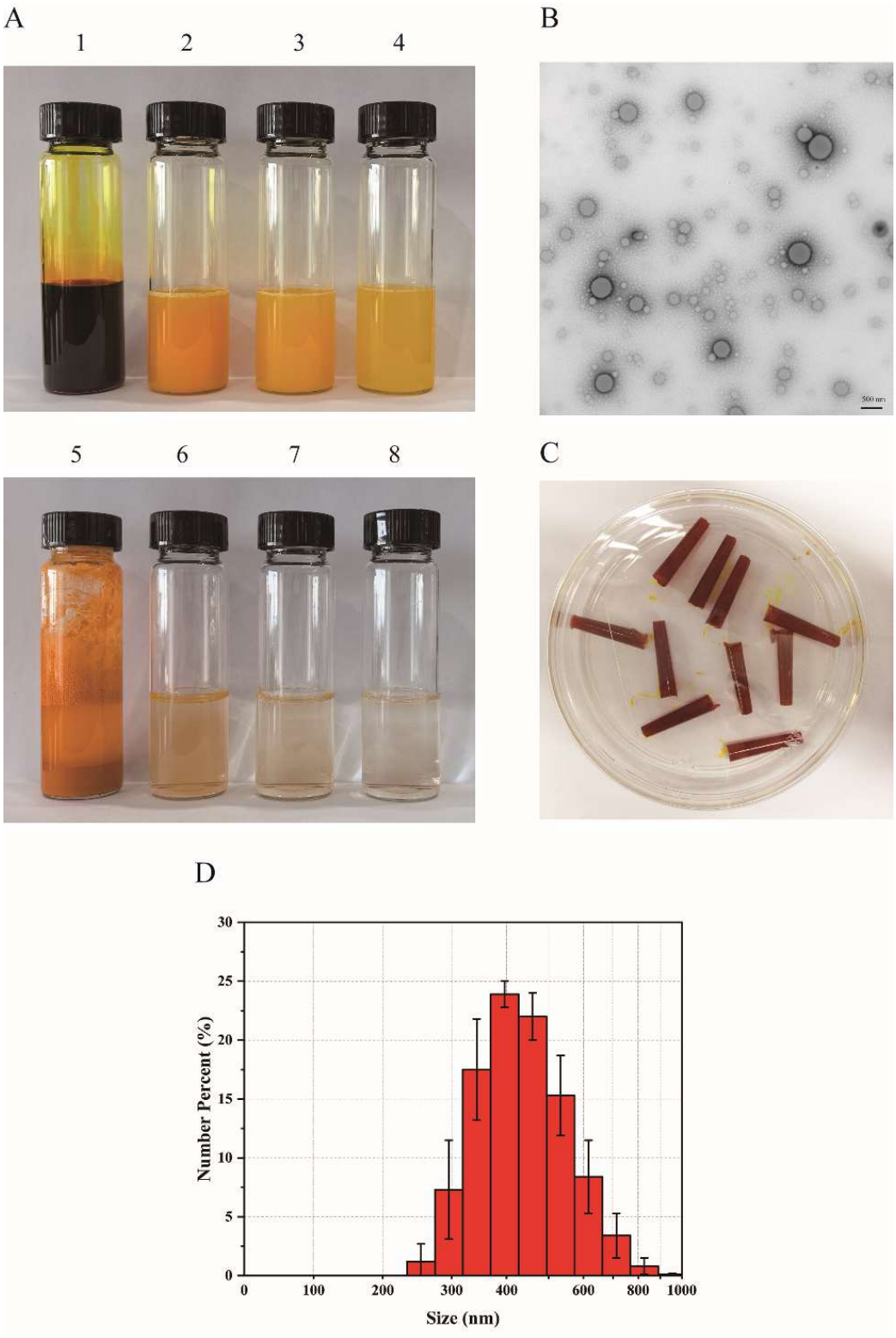

Fig. 3: Morphology of CNG/CS and their dilutions in water.
A: 80 mg/mL curcumin CNG and CS, and their water dilutions were prepared. 1, CNG; 2, CNG water dilution (curcumin 3.2 mg/mL); 3, CNG water dilution (curcumin 1.6 mg/mL); 4, CNG water dilution (curcumin 0.8 mg/mL).; 5, CS; 6, CS water dilution (curcumin 3.2 mg/mL); 7, CS water dilution (curcumin 1.6 mg/mL); 8, CS water dilution (curcumin 0.8 mg/mL). B: TEM micrograph of CNG water solution. The morphology of the aqueous solution of CNG (0.26 mg/mL) was taken by an FEI Tecnai G2 Spirit transmission electron microscope. C: The rectal suppository of solid CNG. D: Particle size distribution of CNG water dilution.

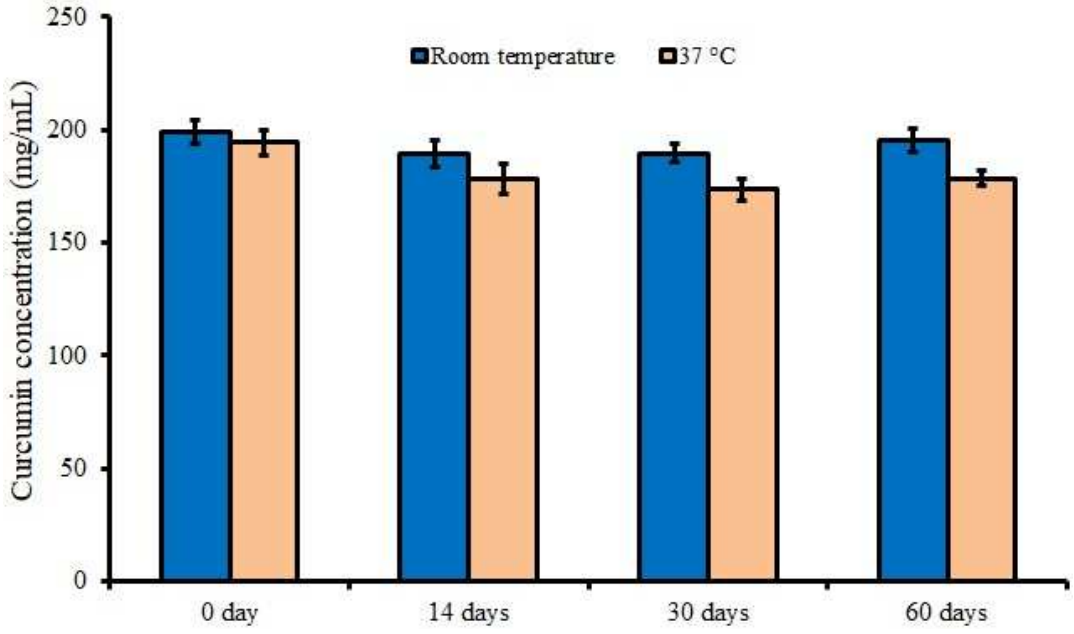

Fig. 4: The stability of curcumin in CNG. The data were presented as the mean ± SD of the triplicates determination.

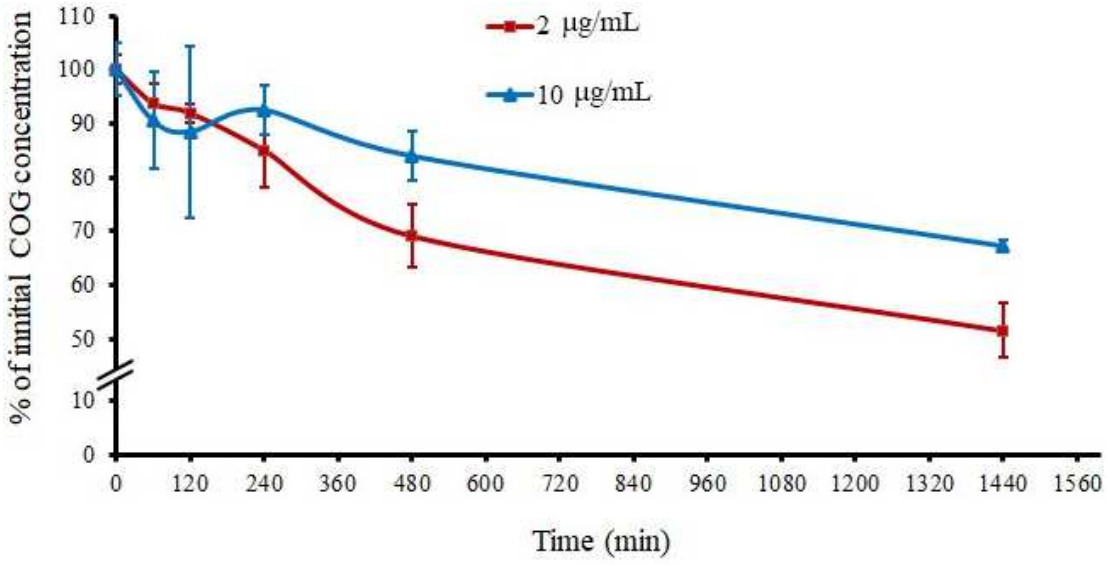

Fig. 5: The stability of COG in mouse plasma: COG (2 and 10 µg/mL) was incubated in mouse plasma at 37°C water bath and COG content was determined by the LC-MS/MS method. The data were presented as the mean ± SD of the triplicates determination.

Table 2: Cytotoxicity of curcumin as CNG and DMSO Solution against cancer cell lines.

Formulation	IC_{50}[a] (µM)		
	MCF-7	MDA-MB-231	MV4-11
DMSO	27.33 ± 1.53	24.67 ± 0.58	4.60 ± 1.59
CNG	23.00 ± 4.00	22.00 ± 1.00	3.30 ± 0.92

[a]IC_{50}: Drug concentration required to reduce cellular proliferation by 50%. It was determined following 72-hour exposure to various curcumin formulations. Cell viability was determined via the MTS colorimetric assay, with IC_{50} values derived from dose-response curves. Results are presented as mean ±SD from triplicate independent experiments.

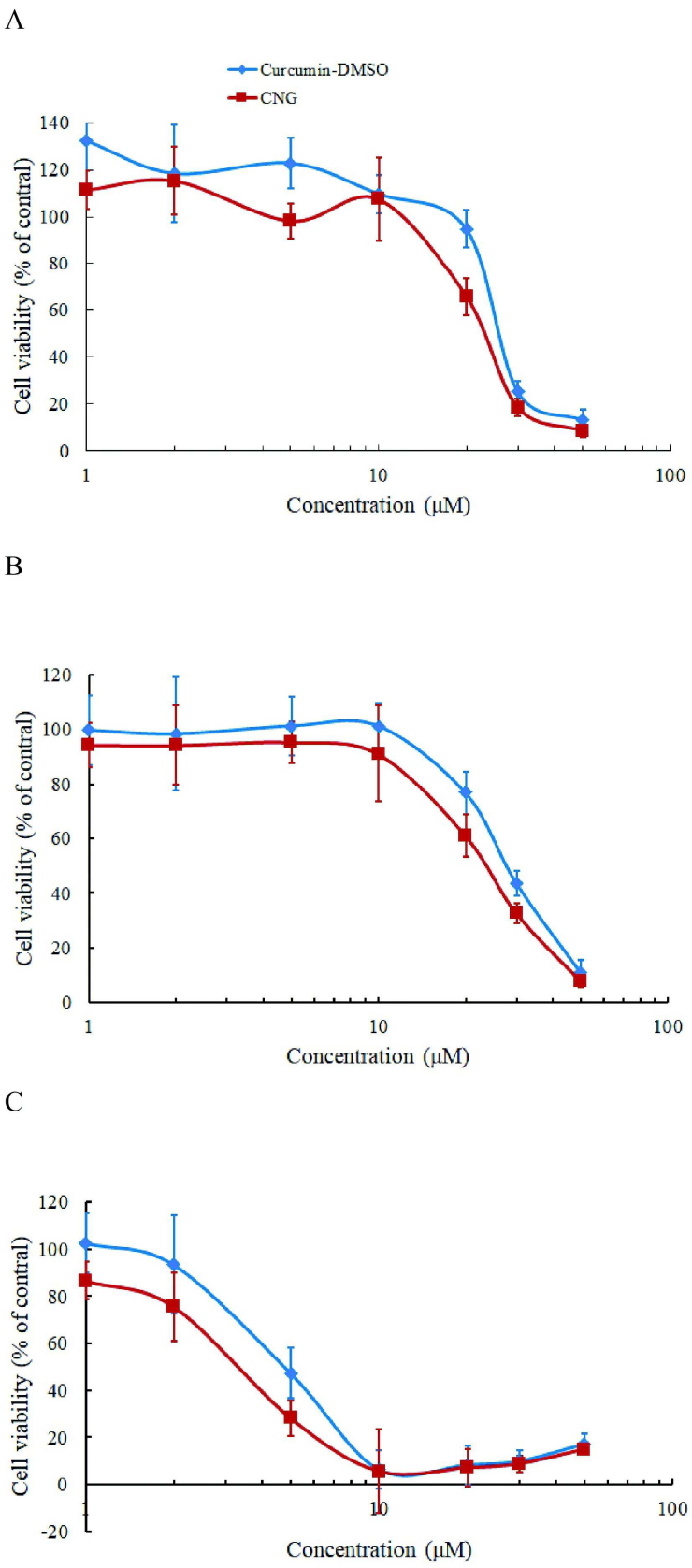

Fig. 6: The dose-response curves of curcumin in CNG and DMSO against human cancer cells. (A) MDA-MB-231, (B) MCF-7 and (C) MV4-11. The data were presented as the mean ± SD of the triplicates determination.

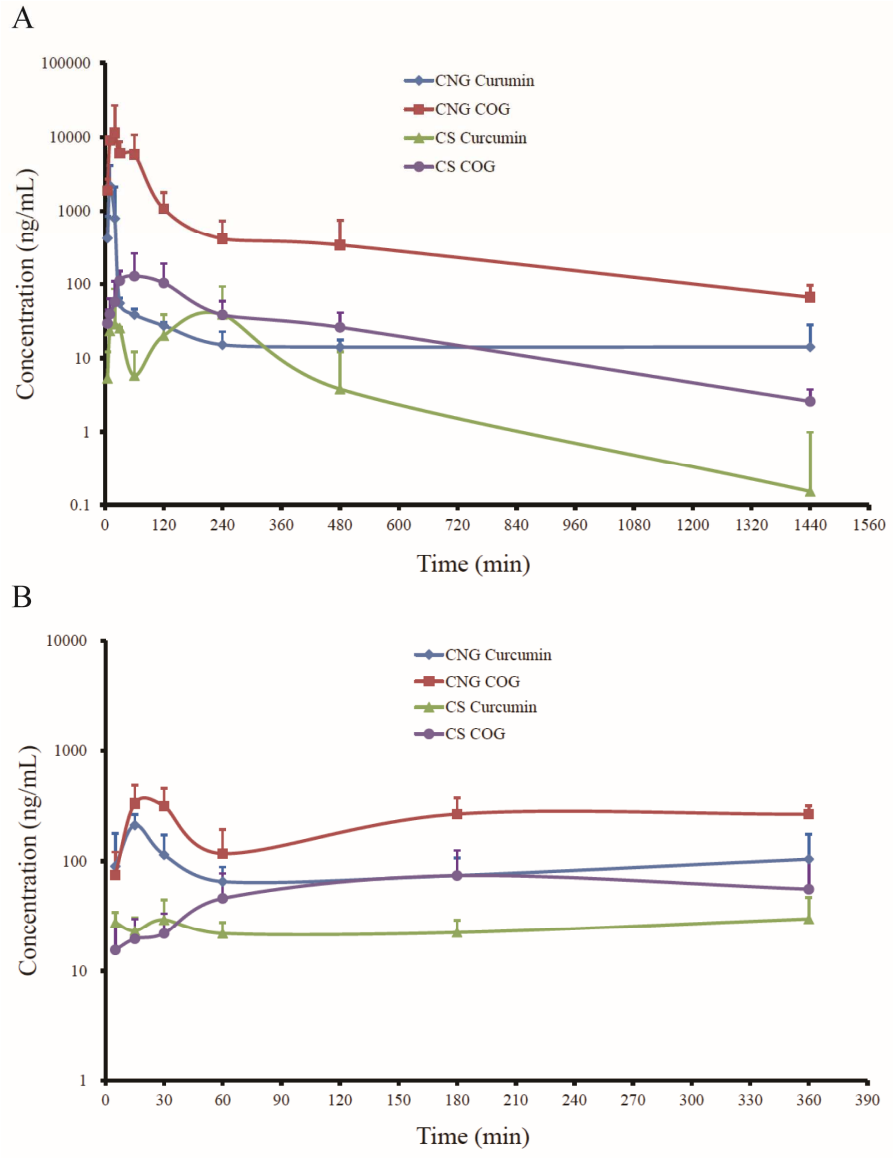

Fig. 7: Plasma concentration-time profile of curcumin and COG *in vivo*.
(A) A single oral administration of CNG and CS formulations (1000 mg/kg; n = 6) in mice. (B) A single rectal suppository administration of CNG and oral administration of CS (200 mg/kg; n = 5) in rats. The data were presented as the mean ± SEM.

Table 3: Pharmacokinetics parameters of curcumin and COG after oral administration of 1000 mg/kg curcumin as CNG and CS.

Parameters	Units	Curcumin (CNG)	Curcumin (CS)	Ratio CNG:CS	COG (CNG)	COG (CS)	Ratio CNG:CS
λ_z	1/min	0.0022	0.0026	0.846	0.0023	0.83	0.003
HL-λ_z	min	318.1	262.4	1.212	367.3	301.7	1.217
T_{max}	min	10.0	240	0.042	10.0	60.0	0.167
C_{max}	µM	7.019	0.1052	66.721	20.1	0.237	84.810
C_{last}	µM	0.0383	0.0026	14.731	0.1226	0.0047	26.085
$AUC_{0\text{-}24hr}$	min×µM	319	34.57	9.228	1897	77.7	24.414
AUC_{INF_obs}	min×µM	337	35.57	9.474	1962	79.7	24.617
$Vz_{\_F\ obs}$	L/kg	3701.5	28895	0.128	733.3	14822	0.049
$Cl_{\_F\ obs}$	L/min/kg	8.07	76.3	0.106	1.38	34.1	0.040

Table 4: Pharmacokinetics parameters of curcumin and COG after rectal administration of 200 mg/kg curcumin as CNG and oral administration of 200 mg/kg curcumin as CS.

Parameters	Units	Curcumin (CNG)	Curcumin (CS)	Ratio CNG:CS	COG (CNG)	COG (CS)	Ratio CNG:CS
λ_z	1/min	0.0048	0.0015	3.200	0.0019	0.0048	0.396
HL-λ_z	min	306.9	629.8	0.487	422.4	289.6	1.459
T_{max}	min	13	162	0.080	123	181	0.680
C_{max}	μM	0.639	0.117	5.462	0.757	0.158	4.791
C_{last}	μM	0.2837	0.0813	3.490	0.4904	0.1029	4.766
$AUC_{0\text{-}6hr}$	min×μM	85.2	24.1	3.535	156.06	37.71	4.138
AUC_{INF_obs}	min×μM	187.65	61.23	3.065	466.67	119.17	3.916
$Vz_{\_F\_obs}$	L/kg	1056	7406.4	0.143	721.7	1980.3	0.364
$Cl_{\_F\_obs}$	L/min/kg	3.7	9.4	0.394	1.3	9.4	0.138

Pharmacokinetic parameters were derived from individual mouse data. These results clearly demonstrate that CNG serves as a highly effective delivery system, achieving pharmacologically relevant plasma concentrations and significantly enhanced oral bioavailability compared to the conventional CS formulation.

Pharmacokinetics analysis of rectal suppository administered CNG in rats

The pharmacokinetic evaluation of solid CNG administered as a rectal suppository at a dose of 200 mg/kg curcumin in SD rats demonstrated superior performance compared to orally administered CS (Fig. 7, Table 3; pharmacokinetic parameters were derived from individual rats). Based on LC-MS/MS analysis, CNG showed a 3.5-fold higher systemic exposure, with an $AUC_{(0\rightarrow6h)}$ of 85.2 μM·min compared to 24.1 μM·min for CS and a 5.5-fold increase in C_{max} (0.64 μM vs. 0.12 μM). Additionally, a similar enhancement in pharmacokinetic parameters was observed for COG in the CNG rectal suppository group, indicating that rectal suppository CNG can enhance the bioavailability of curcumin in rats.

DISCUSSION

Extensive preclinical and clinical evidence supports the broad therapeutic potential of curcumin; however, its pharmacological application is fundamentally limited by exceptionally poor oral bioavailability, which restricts the achievement of effective systemic concentrations required for its documented biological effects (Wang *et al*., 2020). To address this, various novel formulations-such as liposomal curcumin, nanoparticle-based curcumin (Bisht *et al*., 2007, Yallapu *et al*., Mohanty and Sahoo, Gao *et al*., Shahani *et al*., Mohanty *et al*., Mach *et al*., Gota *et al*., Mukerjee and Vishwanatha, 2009, Onoue *et al*.), solid dispersions (SD) curcumin (Xu *et al*., 2008), alginate nano-micelle-loaded curcumin (Zhang and Zhang, 2021), nanocapsulated curcumin (Shan *et al*., 2022) and self-microemulsified (SME) curcumin (Cui *et al*., 2008) have been developed to improve the pharmacokinetic and pharmacological profile of curcumin. While some polyethylene glycols (PEGs) have been reported to solubilize curcumin up to 250 mg/mL and exhibit high loading capacity in mixtures with Cremophor EL (Zhongfa *et al*., 2012). However, cell cytotoxicity study demonstrated that cremophor EL can antagonize the cytotoxicity of curcumin. Therefore, in the present study, an improved curcumin nano-gel (CNG) was successfully formulated using a blend of PEG600 and Tween 20. This CNG formulation demonstrated cytotoxic activity comparable to or better than conventional DMSO-dissolved curcumin across several human cancer cell lines, including breast cancer lines (MCF-7 and MDA-MB-231) and the leukemia cell line MV4-11. Further studies in tumor-bearing xenograft models are warranted to quantitatively evaluate this enhanced cytotoxicity and related PK/PD outcomes, thereby assessing the translational relevance of CNG-induced systemic exposure.

A precise and specific LC-MS/MS method was developed on a triple-quadrupole mass spectrometer and fully validated for simultaneous quantification of curcumin and COG in mouse plasma. Acidification of plasma samples with low-pH phosphate buffer prior to extraction improved both analyte stability and recovery. Current pharmacological understanding suggests that unbound plasma curcumin represents the biologically active species and serves as the most reliable indicator for assessing bioavailability and bioequivalence (Kanae *et al*., 2022). Consistent with previous reports, our results showed characteristically low circulating levels of native curcumin (CS: 0-29 ng/mL; CNG: 0-2209 ng/mL) alongside substantially higher concentrations of its primary metabolite COG (CS: 0-129 ng/mL; CNG: 0-9057 ng/mL), underscoring the extensive first-pass metabolism that limits curcumin's therapeutic utility. COG was detected as early as curcumin, indicating that glucuronide conjugate of curcumin was formed very rapidly. COG may also serve as a sensitive marker of curcumin absorption when parent compound concentrations fall below the detection limit.

Some other types of curcumin formulations, such as Curcumin-loaded nano-liposome (Jang *et al*., 2024),

nanoparticles of curcumin encapsulated in PLGA (Szymusiak *et al*., 2016), CUR-silk nanoparticles (Wu *et al*., 2018) and curcumin-phospholipid complex nanoparticles (Zhang *et al*., 2025) were orally administered to mice or rats and the produced pharmacokinetics outcomes for curcumin and COG was comparable to those of CNG. The CNG formulation developed herein exhibited significantly enhanced absorption compared to conventional curcumin suspension. This improvement likely stems from several mechanisms: PEG-mediated solubilization promotes the formation of a homogeneous solution, (Zhongfa *et al*., 2012) and upon dilution, nanoscale curcumin particles with improved absorption properties are generated. Additionally, Tween 20 and PEG may enhance intestinal membrane permeability and particle-membrane interactions. Curcumin undergoes extensive hepatic first-pass metabolism, primarily via glucuronidation (yielding COG) and sulfation, resulting in metabolites with reduced bioactivity compared to the parent compound (Hassanzadeh *et al*., 2020b, Sharma *et al*., 2007). The liver has been identified as the primary site of curcumin metabolic degradation. In humans, the reported COG-to-curcumin ratio exceeds 20:1. In the present study, based on AUC values, the COG-to-curcumin ratios were approximately 6:1 for oral CNG and 2:1 for rectal CNG, suggesting that the CNG formulation may partially circumvent hepatic first-pass metabolism. Further investigations-such as hepatic portal vein sampling, in situ perfusion, or intestinal permeability assays-are warranted to validate the reduction in first-pass metabolism associated with CNG.

Rectal suppository formulations of CNG represent a promising administration route for curcumin. In addition, the physical stability of curcumin in CNG was evaluated over a two-month period at room temperature and 37°C. The results indicated that CNG possesses good shelf-life stability, with only minimal decomposition observed during extended storage. The pharmacological properties of curcumin have been substantially boosted through innovative nano-sized strategies (Jacob *et al*., 2024). The favorable stability and enhanced pharmacokinetic properties position CNG as a promising delivery system for improving the *in vivo* performance of curcumin.

CONCLUSION

A sensitive LC-MS/MS method was developed and fully validated for the simultaneous quantification of curcumin and its major metabolite, COG, in mouse plasma. The LLOQ were established at 1 ng/mL for curcumin and 2 ng/mL for COG. The method demonstrated excellent precision and accuracy in both intra-day and inter-day validation studies, meeting all FDA GLP requirements for bioanalytical method validation. This robust analytical approach enabled reliable detection of both analytes in plasma samples collected for up to 24 hours following oral administration of CNG or CS formulations at a dose of 1000 mg/kg curcumin equivalents. The developed LC-MS/MS method was subsequently applied to compare the pharmacokinetics of curcumin and COG after administration of CNG and CS, in order to evaluate the oral absorption enhancement afforded by the nano-gel formulation. Pharmacokinetic comparisons revealed that CNG yielded significantly higher peak plasma concentrations (C_{max}) and greater systemic exposure (AUC) of curcumin relative to CS. These results confirm that CNG represents a novel and effective formulation capable of significantly improving the oral absorption and bioavailability of curcumin.

Acknowledgments
Not applicable.

Authors' contributions
Conceptualization, W.C.; methodology, L.H., R.M., X.C. and Z.Y.; software, W.C.; validation, L.H., R.M., X.C. and Z.Y.; formal analysis, L.H., R.M. and D.S.; investigation, L.H., X.C. and W.C.; resources, W.C.; data curation, W.C.; writing-original draft preparation, L.H and W.C.; writing-review and editing, R.M. and W.C.; supervision, W.C.; project administration, W.C.; funding acquisition, W.C.

Funding
This research was funded by National Natural Science Foundation of China (82474120), Zhejiang Province Traditional Chinese Medicine Technology Project (2025ZL213), Key Laboratory of Prevention, Diagnosis and Therapy of Upper Gastrointestinal Cancer of Zhejiang Province.

Data availability statement
Original data in this study are available from the corresponding author on reasonable requests.

Ethical approval
The animal study was approved by the Institutional Animal Care and Use Committee (IACUC) of Zhejiang Cancer Hospital (Approval No: 2023-02-001).

Conflicts of interest
There is no conflict of interest.

Supplementary Data
https://www.pjps.pk/uploads/2026/03/SUP1774695355.pdf

REFERENCES

Bisht S, Feldmann G, Soni S, Ravi R, Karikar C, Maitra A and Maitra A (2007). Polymeric nanoparticle-encapsulated curcumin ("nanocurcumin"): A novel strategy for human cancer therapy. *J. Nanobiotechnology,* **5**: 3.

Cui J, Yu B, Zhao Y, Zhu W, Li H, Lou H and Zhai G

(2009). Enhancement of oral absorption of curcumin by self-microemulsifying drug delivery systems. *Int. J. Pharm*., **371**(1-2): 148-55

Fu YS, Chen TH, Weng L, Huang L, Lai D and Weng CF (2021). Pharmacological properties and underlying mechanisms of curcumin and prospects in medicinal potential. *Biomed. Pharmacother.,* **141**: 111888

Gao Y, Li Z, Sun M, Li H, Guo C, Cui J, Li A, Cao F, Xi Y, Lou H and Zhai G (2010). Preparation, characterization, pharmacokinetics and tissue distribution of curcumin nanosuspension with TPGS as stabilizer. *Drug dev. ind. pharm.,* **36**: 1225-1234.

Gong Y, Wang P, Cao R, Wu J, Ji H, Wang M, Hu C, Huang P and Wang X (2023). Exudate absorbing and antimicrobial hydrogel integrated with multifunctional curcumin-loaded magnesium polyphenol network for facilitating burn wound healing. *ACS Nano,* **17**: 22355-22370.

Gota VS, Maru GB, Soni TG, Gandhi TR, Kochar N and Agarwal MG (2010). Safety and pharmacokinetics of a solid lipid curcumin particle formulation in osteosarcoma patients and healthy volunteers. *J. Agric. Food Chem.,* **58**:2095-2099.

Gupta NK and Dixit VK. (2010). Bioavailability enhancement of curcumin by complexation with phosphatidyl choline. *J. Pharm. Sci*. **100**(5):1987-1995.

Hassanzadeh K, Buccarello L, Dragotto J, Mohammadi A, Corbo M and Feligioni M (2020a). Obstacles against the marketing of curcumin as a Drug. *Int. J. of Mol. Sci.,* **21**(18): 6619.

Hassanzadeh K, Buccarello L, Dragotto J, Mohammadi A, Corbo M and Feligioni M (2020b). Obstacles against the marketing of curcumin as a drug. *Int. J. Mol. Sci.,* **21**(18): 6619.

Heidari H, Bagherniya M, Majeed M, Sathyapalan T, Jamialahmadi, T and Sahebkar A (2023). Curcumin-piperine co-supplementation and human health: A comprehensive review of preclinical and clinical studies. *Phytother. Res.*, **37**(4): 1462-1487.

Jacob S, Kather FS, Morsy MA, Boddu SHS, Attimarad M, Shah J, Shinu P and Nair AB (2024). Advances in nanocarrier systems for overcoming formulation challenges of curcumin: *Current Insights. Nanomaterials (Basel)*, **14**(8): 672.

Jang GH, Kim YM, Kim DH, Shin JW, Yoon SY, Bae JW, Choi JH and Yoon MS (2024). A chitosan/alginate coated nano-liposome to improve intestinal absorption of curcumin for oral administration. *Food Sci. Biotechnol.*, **33**(7): 1707-1714.

Kanae H, Teshima K, Shiroma T and Noguchi K (2022). Pharmacokinetics of a single dose of novel curcumin formulations mixed with fish oils in healthy humans. *Biosci. Biotechnol. Biochem.*, **86**(12): 1688-1694.

Kharat M, Du Z, Zhang G and McClements DJ (2017). Physical and chemical stability of curcumin in aqueous solutions and emulsions: Impact of pH, temperature, and molecular environment. *J. Agric. Food Chem.*, **65**(8): 1525-1532.

Li H, Sureda A, Devkota HP, Pittalà V, Barreca D, Silva AS, Tewari D, Xu S and Nabavi SM (2020). Curcumin, the golden spice in treating cardiovascular diseases. *Biotechnol. Adv.*, **38**: 107343.

Li Y, Zou Q, Yuan C, Li S, Xing R and Yan X (2018). Amino acid coordination driven self‐assembly for enhancing both the biological stability and tumor accumulation of curcumin. Angew. Chem. *Int. Ed*., **57**(52): 17084-17088.

Lübtow MM, Hahn L, Haider MS and Luxenhofer R (2017). Drug specificity, synergy and antagonism in ultrahigh capacity poly(2-oxazoline)/Poly(2-oxazine) based formulations. *J. Am. Chem. Soc.*, **139**(32): 10980-10983.

Ma Z, Wang N, He H and Tang X (2019). Pharmaceutical strategies of improving oral systemic bioavailability of curcumin for clinical application. *J. Controlled Release*, **316**: 359-380.

Mach CM, Chen JH, Mosley SA, Kurzrock R and Smith JA (2010). Evaluation of liposomal curcumin cytochrome p450 metabolism. *Anticancer Res.*, **30**(3): 811-814

Maleki Dizaj S, Alipour M, Dalir Abdolahinia E, Ahmadian E, Eftekhari A, Forouhandeh H, Rahbar Saadat Y, Sharifi S and Zununi Vahed S (2022). Curcumin nanoformulations: Beneficial nanomedicine against cancer. *Phytother. Res.*, **36**(3): 1156-1181.

Mohanty C, Acharya S, Mohanty AK, Dilnawaz F and Sahoo SK (2010). Curcumin-encapsulated MePEG/PCL diblock copolymeric micelles: A novel controlled delivery vehicle for cancer therapy. *NANOMEDICINE-UK*, **5**(3): 433-449.

Mohanty C and Sahoo SK (2010). The *in vitro* stability and *in vivo* pharmacokinetics of curcumin prepared as an aqueous nanoparticulate formulation. *Biomaterials*, **31**(25): 6597-6611.

Mukerjee A and Vishwanatha JK (2009). Formulation, characterization and evaluation of curcumin-loaded PLGA nanospheres for cancer therapy. *Anticancer Res.*, **29**(10): 3867-3875.

Onoue S, Takahashi H, Kawabata Y, Seto Y, Hatanaka J, Timmermann B and Yamada S (2010a). Formulation design and photochemical studies on nanocrystal solid dispersion of curcumin with improved oral bioavailability. *J. Pharm. Sci.*, **99**(4): 1871-1881.

Onoue S, Takahashi H, Kawabata Y, Seto Y, Hatanaka J, Timmermann B and Yamada S (2010b). Formulation design and photochemical studies on nanocrystal solid dispersion of curcumin with improved oral bioavailability. *J. Pharm. Sci.*, **99**(4): 1871-1881.

Pei J, Palanisamy CP, Natarajan PM, Umapathy VR, Roy JR, Srinivasan GP, Panagal M and Jayaraman S (2024). Curcumin-loaded polymeric nanomaterials as a novel therapeutic strategy for Alzheimer's disease: A comprehensive review. *Ageing. Res. Rev.*, **99**: 102393.

Pooresmaeil M and Namazi H (2020). Facile preparation

of pH-sensitive chitosan microspheres for delivery of curcumin; characterization, drug release kinetics and evaluation of anticancer activity. *Int. J. Biol. Macromol.*, **162**: 501-511.

Pourbagher-Shahri AM, Farkhondeh T, Ashrafizadeh M, Talebi M and Samargahndian S (2021). Curcumin and cardiovascular diseases: Focus on cellular targets and cascades. *Biomed. Pharmacother.*, **136**: 111214.

Scazzocchio B, Minghetti L and D'Archivio M (2020). Interaction between gut microbiota and curcumin: A new key of understanding for the health effects of Curcumin. *Nutrients.*, **12**(9): 2499.

Shahani K, Swaminathan SK, Freeman D, Blum A, Ma L and Panyam J (2010). Injectable sustained release microparticles of curcumin: A new concept for cancer chemoprevention. *Cancer Res.*, **70**(11): 4443-4452.

Shan M, Meng F, Tang C, Zhou L, Lu Z and Lu Y (2022). Surfactin effectively improves bioavailability of curcumin by formation of nano-capsulation. *Colloids. Surf. B Biointerfaces.*, **215**: 112521.

Sharma RA, Steward WP and Gescher AJ (2007). Pharmacokinetics and pharmacodynamics of curcumin. *Adv. Exp. Med. Biol.*, **595**: 453-470.

Song Z, Feng R, Sun M, Guo C, Gao Y, Li L and Zhai G (2011). Curcumin-loaded PLGA-PEG-PLGA triblock copolymeric micelles: Preparation, pharmacokinetics and distribution *in vivo*. *J. Colloid. Interface. Sci.*, **354**(1): 116-123.

Szymusiak M, Hu X, Leon Plata PA, Ciupinski P, Wang ZJ and Liu Y (2016). Bioavailability of curcumin and curcumin glucuronide in the central nervous system of mice after oral delivery of nano-curcumin. *Int. J. Pharm.*, **511**(1): 415-423.

Vareed SK, Kakarala M, Ruffin MT, Crowell JA, Normolle DP, Djuric Z and Brenner DE (2008). Pharmacokinetics of curcumin conjugate metabolites in healthy human subjects. *Cancer Epidemiol. Biomarkers Prev.*, **17**: 1411-1417.

Vijaya Saradhi UV, Ling Y, Wang J, Chiu M, Schwartz EB, Fuchs JR, Chan KK and Liu Z (2010). A liquid chromatography-tandem mass spectrometric method for quantification of curcuminoids in cell medium and mouse plasma. *J Chromatogr. B. Analyt. Technol. Biomed. Life Sci.*, **878**(30): 3045-3051.

Wang L, Li W, Cheng D, Guo Y, Wu R, Yin R, Li S, Kuo HC, Hudlikar R, Yang H, Buckley B and Kong AN (2020). Pharmacokinetics and pharmacodynamics of three oral formulations of curcumin in rats. *J. Pharmacokinet. Pharmacodyn.*, **47**(2): 131-144.

Wang W, Li M, Wang L, Chen L and Goh BC (2023). Curcumin in cancer therapy: Exploring molecular mechanisms and overcoming clinical challenges. *Cancer Lett.*, **570**: 216332.

Wei XQ, Zhu JF, Wang XB and Ba K (2020). Improving the stability of liposomal curcumin by adjusting the inner aqueous chamber ph of liposomes. *ACS Omega*, **5**(2): 1120-1126.

Wu J, Wang J, Zhang J, Zheng Z, Kaplan DL, Li G and Wang X (2018). Oral delivery of curcumin using silk nano- and microparticles. *ACS Biomater. Sci. Eng.*, **4**(11): 3885-3894.

Xu DH, Wang S, Mei XT, Luo XJ and Xu SB (2008). Studies on solubility enhancement of curcumin by Polyvinylpyrrolidione K30. *Zhong Yao Cai*, **31**(3): 438-442.

Yallapu MM, Gupta BK, Jaggi M and Chauhan SC (2010). Fabrication of curcumin encapsulated PLGA nanoparticles for improved therapeutic effects in metastatic cancer cells. *J. Colloid. Interface Sci.*, **351**(1): 19-29.

Yavarpour-Bali H, Ghasemi-Kasman M and Pirzadeh M (2019). Curcumin-loaded nanoparticles: A novel therapeutic strategy in treatment of central nervous system disorders. Int. *J. Nanomedicine*, **14**: 4449-4460.

Zhang B, Guo W, Chen Z, Chen Y, Zhang R, Liu M, Yang J and Zhang J (2025). Physicochemical characterization and oral bioavailability of curcumin-phospholipid complex nanosuspensions prepared based on microfluidic system. *Pharmaceutics,* **17**(3): 395.

Zhang L, Qiang P, Yu J, Miao Y, Chen Z, Qu J, Zhao Q, Chen Z, Liu Y, Yao X, Liu B, Cui L, Jing H and Sun G (2018). Identification of compound CA-5f as a novel late-stage autophagy inhibitor with potent anti-tumor effect against non-small cell lung cancer. *Autophagy*, **15**(3): 391-406.

Zhang Y, Rauf Khan A, Fu M, Zhai Y, Ji J, Bobrovskaya L and Zhai G (2019). Advances in curcumin-loaded nanopreparations: Improving bioavailability and overcoming inherent drawbacks. *J. Drug Target*, **27**(9): 917-931.

Zhang Z and Zhang X (2021). Curcumin loading on alginate nano-micelle for anti-infection and colonic wound healing. *J. Biomed. Nanotechnol.*, **17**(6): 1160-1169.

Zhongfa L, Chiu M, Wang J, Chen W, Yen W, Fan-Havard P, Yee LD and Chan KK (2012). Enhancement of curcumin oral absorption and pharmacokinetics of curcuminoids and curcumin metabolites in mice. *Cancer Chemother. Pharmacol.*, **69**(3): 679-689.

Zoi V, Kyritsis AP, Galani V, Lazari D, Sioka C, Voulgaris S and Alexiou GA (2024). The role of curcumin in cancer: A focus on the PI3K/Akt pathway. *Cancers*, **16**(8): 1554.